

An unusual two-dimensional MOF formed from Ni^{II}, thiophene-2,5-dicarboxylate and *trans*-1,2-bis(pyridin-4-yl)ethylene

Chongting Ren, Xu Jia and Luc Van Meervelt*

Department of Chemistry, KU Leuven, Biomolecular Architecture, Celestijnenlaan 200F, Leuven (Heverlee), B-3001, Belgium. *Correspondence e-mail: Luc.VanMeervelt@kuleuven.be

Received 12 January 2026

Accepted 2 March 2026

Edited by F. Di Salvo, University of Buenos Aires, Argentina

Keywords: crystal structure; metal-organic framework; nickel; thiophene-2,5-dicarboxylate; *trans*-1,2-bis(pyridin-4-yl)ethylene.

CCDC reference: 2534227

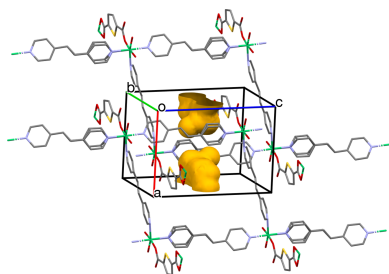
Supporting information: this article has supporting information at journals.iucr.org/e

A new Ni^{II} MOF, poly[[sesqui[μ -*trans*-1,2-bis(pyridin-4-yl)ethylene](μ -thiophene-2,5-dicarboxylato)nickel(II)] dimethylformamide 0.205-solvate], $\{[\text{Ni}(\text{C}_6\text{H}_3\text{O}_4\text{S})(\text{C}_{12}\text{H}_{10}\text{N}_2)_{1.5}].0.205\text{C}_3\text{H}_7\text{NO}]_n\}$, was obtained under solvothermal conditions and its structure was determined by single-crystal X-ray diffraction. The structure reveals that Ni nodes are bridged by thiophene-2,5-dicarboxylate (HT) and *trans*-1,2-bis(pyridin-4-yl)ethylene (Bpe) to generate an unusual two-dimensional layered framework, and the overall crystal is formed by an interlocked stacking of these layers. Topological simplification classifies the framework as a non-interpenetrated 3-nodal (2,2,5)-connected net, in which the Ni-containing node acts as the higher-connected vertex and the two organic ligands serve as 2-connected linkers propagating the connectivity within the layer. The experimental powder X-ray diffraction (PXRD) pattern is in good agreement with that simulated from the single-crystal structure, further confirming that the powder sample is consistent with the single-crystal model and exhibits good phase purity.

1. Chemical context

Metal-organic frameworks (MOFs) continue to attract strong interest in crystal engineering owing to their high structural tunability and rich topological diversity (Furukawa *et al.*, 2013). This diversity arises primarily from the wide range of coordination numbers and geometries accessible to metal nodes (or clusters), together with the adjustable connectivity, length and conformation of organic linkers (O’Keeffe & Yaghi, 2012). As a result, MOFs can display varied dimensionalities and connectivity patterns, often accompanied by key structural features such as porosity, layered packing and interpenetration. In this context, mixed-ligand strategies provide an efficient route to modulate connectivity and spatial extension by combining complementary coordinating groups, thereby expanding the diversity and accessibility of framework architectures and underlying topologies (Yin *et al.*, 2015).

Within the widely used combination of dicarboxylate and N-donor linker construction method, thiophene-2,5-dicarboxylate (HT) exhibits distinctive features. The thiophene core introduces a sulfur-containing heteroaromatic, π -conjugated motif, so that, in addition to providing robust carboxylate bridges, it may influence interlayer packing and framework dimensionality through π - π interactions and other weak supramolecular contacts (Thuéry & Harrowfield, 2022; Zheng *et al.*, 2008). Meanwhile, the linear N-donor ligand *trans*-1,2-bis(pyridin-4-yl)ethylene (Bpe) is rigid and offers a relatively long spacer length; its terminal pyridyl N atoms



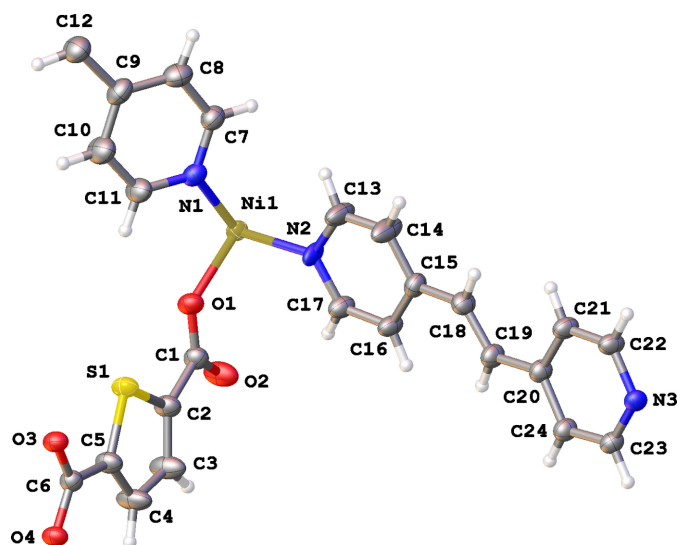


Figure 1
Asymmetric unit of the title compound Ni-HT-Bpe showing the atom labelling and 30% probability ellipsoids. Only the major component of the disordered *trans*-1,2-bis(pyridin-4-yl)ethylene is shown and the partial dimethylformamide molecule has been removed for clarity.

impart well-defined directional coordination and it is therefore frequently employed as a ‘pillar’ to tune metal–metal separations, promote layered architectures, and regulate the underlying topology (Wu *et al.*, 2019; Zhang *et al.*, 2012). Accordingly, the synergistic assembly of HT and Bpe provides a suitable platform for constructing frameworks with characteristic layered motifs and topological features.

On this basis, a new Ni^{II} MOF, Ni-HT-Bpe, was obtained under solvothermal conditions and its structure was determined by single-crystal X-ray diffraction. Notably, the framework adopts a thick parallel polycatenated 2D entangled architecture, which belongs to a comparatively rare subclass among entangled 2D coordination networks (*ca.* 9.2% overall in an extended ring net (ERN)-based statistical survey; Alexandrov *et al.*, 2017). Moreover, closely related systems based on the same (or very similar) linker combinations more commonly form twofold interpenetrated 3D frameworks (Jia *et al.*, 2024; Alamgir *et al.*, 2021; Sen *et al.*, 2013), highlighting an unusual structure–composition relationship for Ni-HT-Bpe.

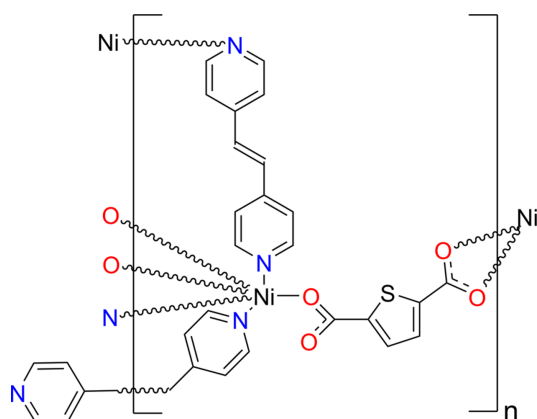


Table 1
Selected bond lengths (Å).

Ni1–O1	2.017 (3)	Ni1–N1	2.094 (3)
Ni1–O3 ⁱ	2.156 (3)	Ni1–N3 ⁱⁱ	2.112 (3)
Ni1–O4 ⁱ	2.144 (3)	Ni1–N2	2.109 (9)

Symmetry codes: (i) $x, y + 1, z$; (ii) $x, y, z - 1$.

Table 2
Hydrogen-bond geometry (Å, °).

*Cg*1, *Cg*2 and *Cg*3 are the centroids of rings (N2A,C13A–C17A), (N3,C20–C24) and (N1,C7–C11), respectively.

<i>D</i> –H··· <i>A</i>	<i>D</i> –H	H··· <i>A</i>	<i>D</i> ··· <i>A</i>	<i>D</i> –H··· <i>A</i>
C8–H8···O2 ⁱⁱⁱ	0.93	2.59	3.314 (7)	135
C19–H19A···O4 ^{iv}	0.93	2.51	3.430 (6)	169
C21–H21···O3 ^v	0.93	2.41	3.331 (6)	171
C27–H27C··· <i>Cg</i> 1	0.96	2.78	3.57 (6)	140
C10–H10··· <i>Cg</i> 2 ^v	0.93	2.88	3.696 (6)	147
C22–H22··· <i>Cg</i> 3 ^{vi}	0.93	2.93	3.534 (5)	124

Symmetry codes: (iii) $x - 1, y, z$; (iv) $-x + 2, -y + 1, -z + 1$; (v) $-x + 1, -y + 1, -z + 1$; (vi) $x, y, z + 1$.

2. Structural commentary

The Ni-HT-Bpe structure crystallizes in the triclinic space group $P\bar{1}$ with one Ni ion, one thiophene-2,5-dicarboxylate and one and a half *trans*-1,2-bis(pyridin-4-yl)ethylene in the asymmetric unit (Fig. 1). The asymmetric unit also contains a dimethylformamide (DMF) molecule with an occupancy of 0.205 (7) close to the inversion center at 1/2,1/2,1/2 generating a second DMF. The second Bpe half is generated by inversion symmetry. The other Bpe molecule is partly disordered (atoms N2, C13–C18) over two positions with occupancies of 0.544 (17) and 0.456 (17).

The Ni ion is octahedrally coordinated by three N atoms from Bpe [atoms N1, N2 and N3($x, y, -1 + z$)] and three O atoms from HT [atoms O1, O3($x, 1 + y, z$) and O4($x, 1 + y, z$)] (Table 1). This results in chain formation in three directions: in the *c*-axis direction by interactions with N2 and N3, close to the *a*-axis direction by interactions with N1, and in the *b*-axis direction by interactions with O1, O3 and O4 (Table 1, Fig. 2). Oxygen atom O2 does not interact with the Ni ion, but forms a hydrogen bond with the neighbouring Bpe pyridyl ring (atom H8, see Table 2). Oxygen atoms O3 and O4 also show

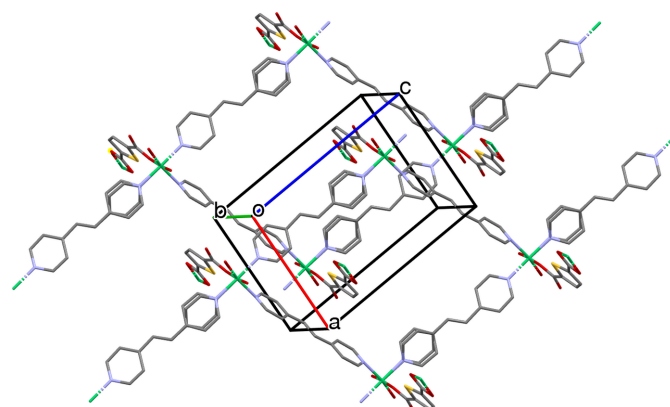


Figure 2
Packing diagram of Ni-HT-Bpe. Hydrogen atoms and DMF molecules are omitted for clarity.

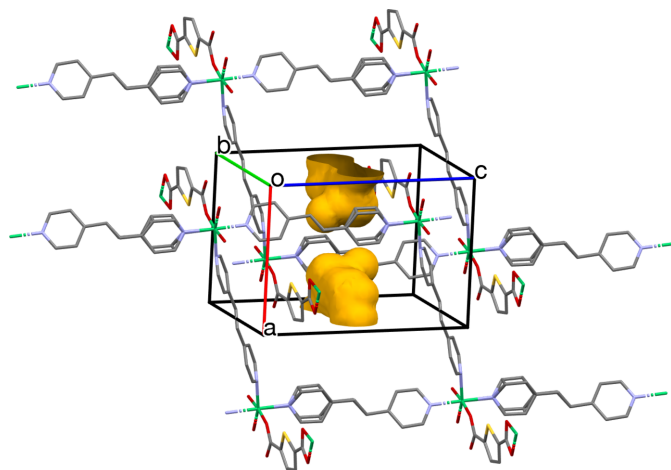


Figure 3
Visualization of the voids in the crystal packing of Ni-HT-Bpe using *Mercury* (Macrae *et al.*, 2020).

hydrogen bonds with the other Bpe molecule (atoms H21 and H19A, respectively, see Table 2).

The DMF molecule is positioned close to the disordered Bpe part and one of the methyl groups interacts with it through a C–H $\cdots\pi$ interaction (Table 2). In addition, a C=O $\cdots\pi$ interaction is observed with a neighbouring (N1, C17–C11) ring. Two additional C–H $\cdots\pi$ interactions are listed in Table 2.

A void-space representation was generated using *Mercury* (Macrae *et al.*, 2020) for the solvent-free structural model (Fig. 3). The plot highlights the presence of internal cavities within the unit cell, which appear as discrete void regions rather than a clearly continuous channel system. A quantitative porosity analysis was carried out using *Zeo++* (Willems *et al.*, 2012) in high-accuracy mode using the solvent-free CIF. The framework exhibits a substantial geometric void volume of 454.2 Å³ per unit cell, corresponding to a void fraction of 0.372. However, the probe-accessible volume and accessible surface area are both zero for a probe radius of 1.86 Å (approximate the kinetic size of N₂) indicating that the pore apertures are too small to be accessible to N₂ under this probe condition.

The structure reveals that Ni nodes are bridged by HT and Bpe to generate an unusual two-dimensional layered framework, and the overall crystal is formed by an interlocked stacking of these layers. Topological simplification classifies the framework as a non-interpenetrated 3-nodal (2,2,5)-connected net, in which the Ni-containing node acts as the higher-connected vertex and the two organic ligands serve as 2-connected linkers propagating the connectivity within the layer. The experimental powder X-ray diffraction (PXRD) pattern is in good agreement with that simulated from the single-crystal structure, further confirming that the powder sample is consistent with the single-crystal model and exhibits good phase purity.

The connectivity of Ni-HT-Bpe was analyzed by a topological simplification in which the coordination framework is reduced to its underlying net (Fig. 4; Blatov *et al.*, 2014). The

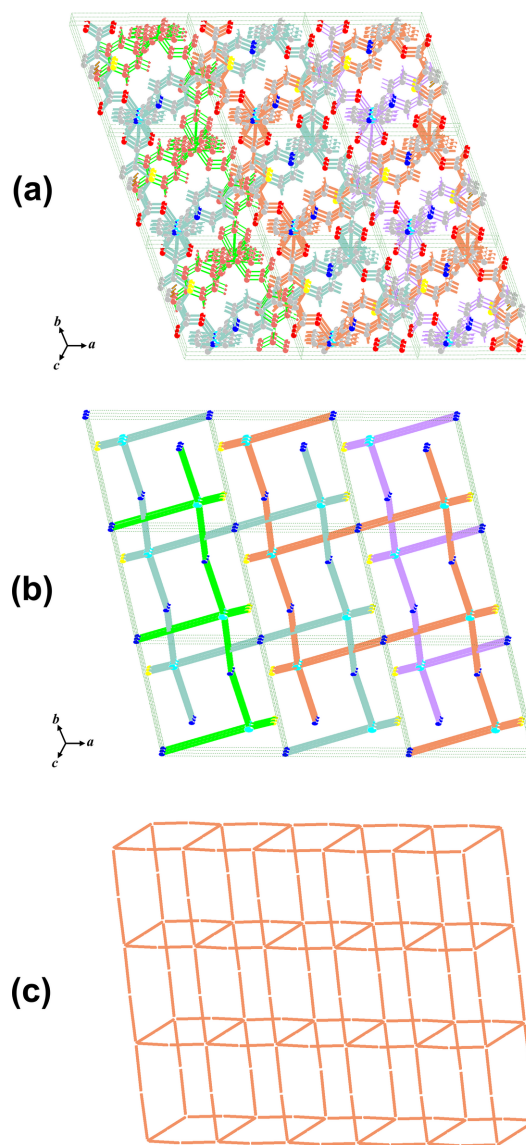


Figure 4
Topological analysis of Ni-HT-Bpe: (a) 3 × 3 × 3 unit cells of the framework; (b) 3 × 3 × 3 unit cells view of the corresponding simplified net; (c) representation of a single two-dimensional layer [parallel to (100)].

structure forms 2D layers parallel to (100), and only one structural group is present, indicating that the framework is non-interpenetrated. In the reduced representation, the layer can be described as a 3-nodal (2,2,5)-connected net. The metal-containing node (originating from the Ni coordination environment) acts as the higher-connected vertex, while both organic linkers function as 2-connected spacers that propagate the network within the layer. The resulting topology is 2²,5-c net with stoichiometry (2-c)₄(2-c)(5-c)₂.

3. Database survey

A search of the Cambridge Structural Database (CSD, version 6.01, November 2025; Groom *et al.*, 2016) for thiophene-2,5-dicarboxylate resulted in 868 hits with 27 containing an O \cdots Ni

interaction of which 20 are present in the MOF subset. A search for 1,2-bis(pyridin-4-yl)ethylene yielded 2868 hits with 123 showing an $N \cdots Ni$ interaction of which 97 hits belong to the MOF subset.

Two structures are worthwhile to mention due to the presence of very similar building units. Refcode LICNER (Han *et al.*, 2007) refers to a Ni polymer containing thiophene-2,5-dicarboxylate (tda) and 1,3-di-pyridin-4-ylpropane (bpp). Each Ni ion is six-coordinated by four O atoms (two from two independent tda and two aqua O atoms) and two N atoms from two bpp ligands. A 2D grid-type bilayer formed through intermolecular $O-H \cdots O$ interactions is running parallel to the (001) plane.

The asymmetric unit of the second one, KIFBOT (Lu *et al.*, 2018), contains one Ni atom, one thiophene-2,5-dicarboxylate anion (tdc), one 2,2'-dimethyl-4,4'-bipyridine ligand (dmbpy) and one μ_2 -O atom. The Ni ion is six-coordinated by three carboxylate O atoms from three different tda, two N atoms from two different dmbpy and one μ_2 -O atom. A dimeric Ni unit $[Ni_2(COO)_4(\mu_2-OH)]$ acts as secondary building unit (SBU) and neighbouring SBUs are connected by tdc ligands to form 2D grids, which extend into a 3D framework by dmbpy pillars.

4. Synthesis and crystallization

The reaction scheme to synthesize the title compound is given in Fig. 5.

$Ni(NO_3)_2 \cdot 6H_2O$ (29 mg, 0.10 mmol), thiophene-2,5-dicarboxylic acid (HT; 15.6 mg, 0.10 mmol) and trans-1,2-bis(pyridin-4-yl)ethylene (Bpe; 27 mg, 0.15 mmol) were placed in a 25 mL Teflon-lined stainless-steel autoclave, and DMF/EtOH/H₂O (10 mL) was added. The mixture was sonicated for 5 min and then stirred at room temperature for 10 min to give a homogeneous suspension. The vessel was sealed and heated at 368K for 4 days and then cooled to room temperature at a rate of 6 K h⁻¹. Green block-shaped crystals and needle-like crystals of Ni-HT-Bpe were obtained. For powder preparation, the as-synthesized product was collected by filtration, washed with DMF (3 × 10 mL) followed by EtOH (3 × 10 mL), and dried in a vacuum oven at 353K overnight to afford Ni-HT-Bpe as green powder (54 mg, 75% yield based on Bpe).

The phase purity of the powder sample was assessed by powder X-ray diffraction (PXRD). Powder X-ray diffraction data were collected on a PANalytical Empyrean diffractometer (Malvern Panalytical) in transmission geometry over

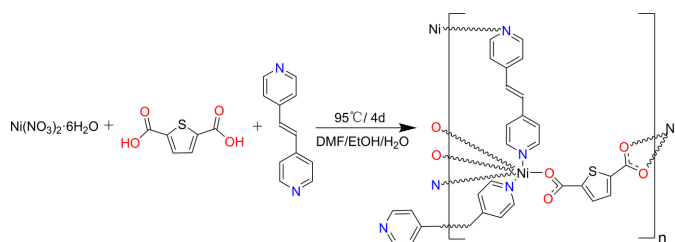


Figure 5
Reaction scheme for the synthesis of Ni-HT-Bpe.

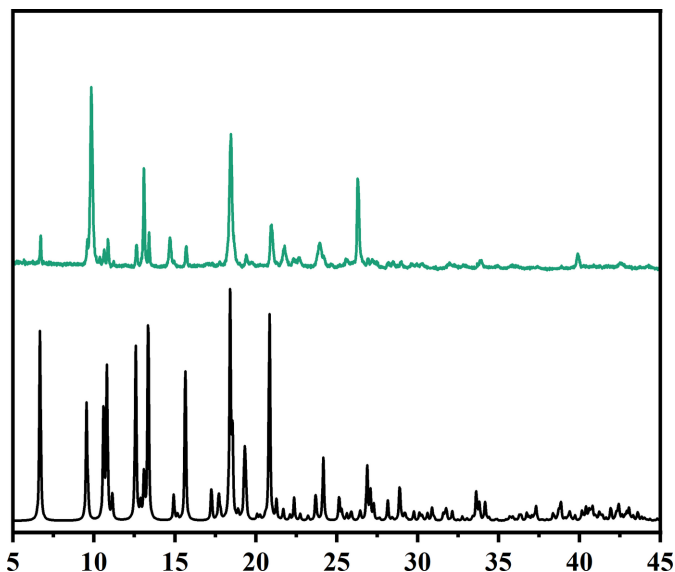


Figure 6
Experimental (top) and simulated (bottom) PXRD patterns of Ni-HT-Bpe. The experimental pattern was recorded using Cu $K\alpha$ radiation, and the simulated pattern was calculated using *Mercury* (Macrae *et al.*, 2020) based on the single-crystal structure.

the 2θ range 1.3–45°, using a PIXcel3D hybrid pixel detector and Cu $K\alpha$ radiation ($K\alpha_1$, $\lambda = 1.5406 \text{ \AA}$; $K\alpha_2$, $\lambda = 1.5444 \text{ \AA}$). The experimental PXRD pattern matches well with the peak positions in the pattern simulated from the single-crystal X-ray structure using *Mercury* (Macrae *et al.*, 2020), confirming that the crystalline powder material is consistent with the single-crystal model (Fig. 6). Noticeable discrepancies in relative intensities are observed. As the sample contains both needle-shaped and block-like crystals (Fig. 7), these discrepancies can be attributed mainly to preferred orientation effects arising from the strongly anisotropic, needle-

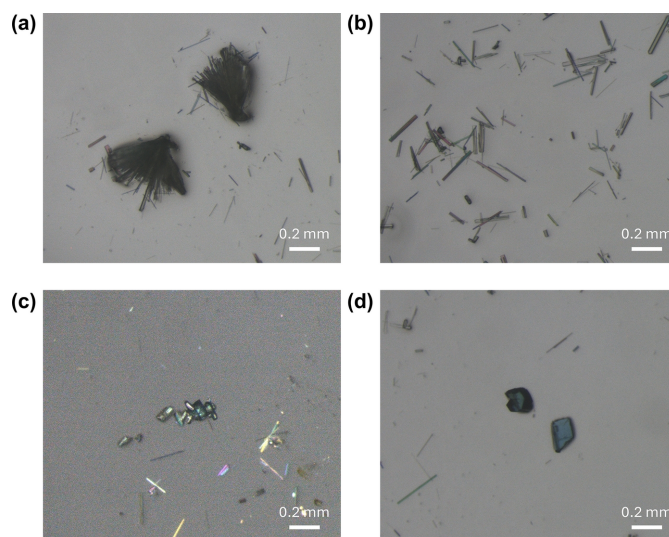


Figure 7
Optical micrographs of needle-like and block-like crystals in the as-synthesized sample (bright-field); panel (c) was acquired under crossed polarizers.

shaped crystallites (and their intergrown bundles) present in the bulk sample, whereas the simulated pattern assumes an ideal randomly oriented powder.

5. Refinement

Crystal data, data collection and structure refinement details are summarized in Table 3. Part of *trans*-1,2-bis(pyridyl) ethylene (atoms N2, C13-C18) was disordered over two positions with occupancies of 0.544 (17) and 0.456 (17). The DMF molecule with refined occupancy 0.205 (7) was subject to DFIX, FLAT, RIGU and ISOR restraints to maintain the expected geometry.

Acknowledgements

CR and XJ acknowledge the China Scholarship Council (CSC) for doctoral fellowships. We thank Professor Tatjana N. Parac-Vogt and Professor Wim Dehaen for access to powder X-ray diffraction facilities and laboratory resources for synthesis. We thank Dongjing Hong (Anhui Normal University, China) for providing access to the X-ray diffractometer. We acknowledge the use of the DIRAC computer cluster (Department of Chemistry, KU Leuven) for computational resources.

References

- Alamgir, Talha, K., Wang, Y.-J., Ullah, R., Wang, B., Wang, L., Wu, W., Chen, S., Xie, L.-H. & Li, J.-R. (2021). *RSC Adv.* **11**, 23838–23845.
- Alexandrov, E. V., Blatov, V. A. & Proserpio, D. M. (2017). *CrystEngComm* **19**, 1993–2006.
- Blatov, V. A., Shevchenko, A. P. & Proserpio, D. M. (2014). *Cryst. Growth Des.* **14**, 3576–3586.
- Bruker (2015). *SAINT*. Bruker AXS Inc., Madison, Wisconsin, USA.
- Dolomanov, O. V., Bourhis, L. J., Gildea, R. J., Howard, J. A. K. & Puschmann, H. (2009). *J. Appl. Cryst.* **42**, 339–341.
- Furukawa, H., Cordova, K. E., O’Keeffe, M. & Yaghi, O. M. (2013). *Science* **341**, 1230444.
- Groom, C. R., Bruno, I. J., Lightfoot, M. P. & Ward, S. C. (2016). *Acta Cryst.* **B72**, 171–179.
- Han, K.-F., Wang, D. & Wang, Z.-M. (2007). *Acta Cryst.* **E63**, m1333–m1334.
- Jia, T., Otake, K., Gu, Y., Nakamura, Y., Kubota, Y., Kawaguchi, S., Wu, J., Li, F. & Kitagawa, S. (2024). *Cryst. Growth Des.* **24**, 9425–9432.
- Krause, L., Herbst-Irmer, R., Sheldrick, G. M. & Stalke, D. (2015). *J. Appl. Cryst.* **48**, 3–10.
- Lu, K., Ma, D.-Y. & Sakiyama, H. (2018). *Inorg. Chem. Commun.* **91**, 39–43.

Table 3

Experimental details.

Crystal data	
Chemical formula	[Ni(C ₆ H ₃ O ₄ S)(C ₁₂ H ₁₀ N ₂) _{1.5}] _{0.205} C ₃ H ₇ NO
<i>M_r</i>	517.08
Crystal system, space group	Triclinic, <i>P</i> $\bar{1}$
Temperature (K)	273
<i>a</i> , <i>b</i> , <i>c</i> (Å)	9.7666 (4), 9.8999 (4), 13.5669 (6)
α , β , γ (°)	98.092 (2), 96.235 (2), 107.823 (2)
<i>V</i> (Å ³)	1220.25 (9)
<i>Z</i>	2
Radiation type	Cu <i>K</i> α
μ (mm ⁻¹)	2.26
Crystal size (mm)	0.15 × 0.13 × 0.12
Data collection	
Diffractometer	Bruker D8 Venture
Absorption correction	Multi-scan (<i>SADABS</i> ; Krause <i>et al.</i> , 2015)
<i>T_{min}</i> , <i>T_{max}</i>	0.487, 0.754
No. of measured, independent and observed [<i>I</i> > 2 σ (<i>I</i>)] reflections	16259, 4801, 3940
<i>R_{int}</i>	0.058
(<i>sin</i> θ / λ) _{max} (Å ⁻¹)	0.620
Refinement	
<i>R</i> [<i>F</i> ² > 2 σ (<i>F</i> ²)], <i>wR</i> (<i>F</i> ²), <i>S</i>	0.066, 0.185, 1.04
No. of reflections	4801
No. of parameters	411
No. of restraints	77
H-atom treatment	H-atom parameters constrained
$\Delta\rho_{\max}$, $\Delta\rho_{\min}$ (e Å ⁻³)	0.43, -0.60

Computer programs: *SAINT* (Bruker, 2015), *SHELXT2018/2* (Sheldrick, 2015a), *SHELXL2016/4* (Sheldrick, 2015b) and *OLEX2* (Dolomanov *et al.*, 2009).

- Macrae, C. F., Sovago, I., Cottrell, S. J., Galek, P. T. A., McCabe, P., Pidcock, E., Platings, M., Shields, G. P., Stevens, J. S., Towler, M. & Wood, P. A. (2020). *J. Appl. Cryst.* **53**, 226–235.
- O’Keeffe, M. & Yaghi, O. M. (2012). *Chem. Rev.* **112**, 675–702.
- Sen, R., Mal, D., Brandão, P., Rogez, G. & Lin, Z. (2013). *CrystEngComm* **15**, 2113–2119.
- Sheldrick, G. M. (2015a). *Acta Cryst.* **A71**, 3–8.
- Sheldrick, G. M. (2015b). *Acta Cryst.* **C71**, 3–8.
- Thuéry, P. & Harrowfield, J. (2022). *Inorg. Chem.* **61**, 9725–9745.
- Willems, T. F., Rycroft, C. H., Kazi, M., Meza, J. C. & Haranczyk, M. (2012). *Microporous Mesoporous Mater.* **149**, 134–141.
- Wu, Y.-P., Tian, J.-W., Liu, S., Li, B., Zhao, J., Ma, L.-F., Li, D.-S., Lan, Y.-Q. & Bu, X. (2019). *Angew. Chem. Int. Ed.* **58**, 12185–12189.
- Yin, Z., Zhou, Y.-L., Zeng, M.-H. & Kurmoo, M. (2015). *Dalton Trans.* **44**, 5258–5275.
- Zhang, P., Liu, Y.-J., Li, K.-H., Yang, G.-R. & Mei, C.-Z. (2012). *Acta Cryst.* **E68**, m1058–m1059.
- Zheng, S.-T., Zhang, J. & Yang, G.-Y. (2008). *Angew. Chem. Int. Ed.* **47**, 3909–3913.

supporting information

Acta Cryst. (2026). E82, 331-335 [https://doi.org/10.1107/S2056989026002276]

An unusual two-dimensional MOF formed from Ni^{II}, thiophene-2,5-dicarboxylate and *trans*-1,2-bis(pyridin-4-yl)ethylene

Chongting Ren, Xu Jia and Luc Van Meervelt

Computing details

Poly[[sesqui[*μ-trans*-1,2-bis(pyridin-4-yl)ethylene](*μ*-thiophene-2,5-dicarboxylato)nickel(II)] dimethylformamide 0.205-solvate]

Crystal data

[Ni(C₆H₃O₄S)(C₁₂H₁₀N₂)_{1.5}].0.205C₃H₇NO

$M_r = 517.08$

Triclinic, $P\bar{1}$

$a = 9.7666$ (4) Å

$b = 9.8999$ (4) Å

$c = 13.5669$ (6) Å

$\alpha = 98.092$ (2)°

$\beta = 96.235$ (2)°

$\gamma = 107.823$ (2)°

$V = 1220.25$ (9) Å³

$Z = 2$

$F(000) = 532$

$D_x = 1.407$ Mg m⁻³

Cu $K\alpha$ radiation, $\lambda = 1.54178$ Å

Cell parameters from 8971 reflections

$\theta = 5.6$ – 72.4 °

$\mu = 2.26$ mm⁻¹

$T = 273$ K

Block, clear light green

$0.15 \times 0.13 \times 0.12$ mm

Data collection

Bruker D8 Venture

diffractometer

Detector resolution: 7.9 pixels mm⁻¹

φ and ω scans

Absorption correction: multi-scan

(SADABS; Krause et al., 2015)

$T_{\min} = 0.487$, $T_{\max} = 0.754$

16259 measured reflections

4801 independent reflections

3940 reflections with $I > 2\sigma(I)$

$R_{\text{int}} = 0.058$

$\theta_{\max} = 73.0$ °, $\theta_{\min} = 5.6$ °

$h = -10$ → 12

$k = -12$ → 12

$l = -16$ → 16

Refinement

Refinement on F^2

Least-squares matrix: full

$R[F^2 > 2\sigma(F^2)] = 0.066$

$wR(F^2) = 0.185$

$S = 1.04$

4801 reflections

411 parameters

77 restraints

Hydrogen site location: inferred from

neighbouring sites

H-atom parameters constrained

$w = 1/[\sigma^2(F_o^2) + (0.0753P)^2 + 2.321P]$

where $P = (F_o^2 + 2F_c^2)/3$

$(\Delta/\sigma)_{\max} < 0.001$

$\Delta\rho_{\max} = 0.43$ e Å⁻³

$\Delta\rho_{\min} = -0.60$ e Å⁻³

Extinction correction: SHELXL-2016/4

(Sheldrick, 2015b),

$F_c^* = kFc[1 + 0.001 \times Fc^2 \lambda^3 / \sin(2\theta)]^{-1/4}$

Extinction coefficient: 0.0106 (15)

Special details

Geometry. All esds (except the esd in the dihedral angle between two l.s. planes) are estimated using the full covariance matrix. The cell esds are taken into account individually in the estimation of esds in distances, angles and torsion angles; correlations between esds in cell parameters are only used when they are defined by crystal symmetry. An approximate (isotropic) treatment of cell esds is used for estimating esds involving l.s. planes.

Fractional atomic coordinates and isotropic or equivalent isotropic displacement parameters (\AA^2)

	<i>x</i>	<i>y</i>	<i>z</i>	$U_{\text{iso}}^*/U_{\text{eq}}$	Occ. (<1)
Ni1	0.69283 (7)	0.86205 (6)	0.22629 (4)	0.0380 (3)	
S1	0.75169 (11)	0.38941 (11)	0.23040 (9)	0.0504 (3)	
O1	0.7559 (3)	0.6858 (3)	0.2229 (2)	0.0504 (7)	
O2	0.9965 (4)	0.7930 (3)	0.2616 (3)	0.0727 (10)	
O3	0.6566 (3)	0.0670 (3)	0.2320 (2)	0.0470 (6)	
O4	0.8783 (3)	0.0550 (3)	0.2622 (2)	0.0459 (6)	
N1	0.4762 (4)	0.7301 (4)	0.1770 (2)	0.0458 (8)	
N3	0.7129 (4)	0.8640 (3)	1.0730 (2)	0.0423 (7)	
C1	0.8847 (5)	0.6871 (4)	0.2486 (3)	0.0485 (9)	
C2	0.8999 (5)	0.5449 (4)	0.2600 (4)	0.0516 (10)	
C3	1.0229 (5)	0.5158 (5)	0.2889 (5)	0.0751 (16)	
H3	1.114325	0.585919	0.307182	0.090*	
C4	0.9981 (5)	0.3673 (5)	0.2886 (5)	0.0744 (16)	
H4	1.071606	0.329647	0.306474	0.089*	
C5	0.8571 (5)	0.2859 (4)	0.2596 (4)	0.0518 (10)	
C6	0.7934 (4)	0.1281 (4)	0.2508 (3)	0.0434 (8)	
C7	0.3659 (5)	0.7815 (5)	0.1773 (3)	0.0537 (10)	
H7	0.382073	0.872090	0.215811	0.064*	
C8	0.2282 (5)	0.7078 (6)	0.1236 (4)	0.0649 (12)	
H8	0.154093	0.748213	0.126837	0.078*	
C9	0.2014 (5)	0.5726 (5)	0.0647 (4)	0.0607 (12)	
C10	0.3152 (6)	0.5201 (6)	0.0651 (5)	0.0744 (15)	
H10	0.302092	0.430102	0.026884	0.089*	
C11	0.4482 (5)	0.5981 (5)	0.1210 (4)	0.0604 (12)	
H11	0.522886	0.558289	0.120386	0.072*	
C12	0.0596 (5)	0.4845 (6)	0.0014 (4)	0.0686 (13)	
H12	0.056538	0.399799	-0.039758	0.082*	
N2a	0.6832 (11)	0.8719 (19)	0.3816 (7)	0.049 (6)	0.544 (17)
C13a	0.5639 (11)	0.877 (2)	0.4220 (7)	0.074 (4)	0.544 (17)
H13a	0.484307	0.881302	0.379870	0.089*	0.544 (17)
C14a	0.5542 (11)	0.876 (2)	0.5208 (6)	0.080 (5)	0.544 (17)
H14a	0.465101	0.865300	0.542590	0.096*	0.544 (17)
C15a	0.6735 (16)	0.889 (2)	0.5887 (9)	0.051 (4)	0.544 (17)
C16a	0.8002 (12)	0.8912 (16)	0.5493 (8)	0.050 (3)	0.544 (17)
H16a	0.883435	0.894223	0.591251	0.060*	0.544 (17)
C17a	0.8004 (13)	0.8888 (16)	0.4472 (9)	0.053 (3)	0.544 (17)
H17a	0.888120	0.899723	0.423208	0.064*	0.544 (17)
C18a	0.660 (2)	0.879 (2)	0.6943 (10)	0.051 (5)	0.544 (17)
H18a	0.568903	0.867991	0.712312	0.062*	0.544 (17)

N12b	0.6761 (16)	0.867 (2)	0.3781 (12)	0.059 (9)	0.456 (17)
C113b	0.5687 (17)	0.762 (2)	0.4074 (8)	0.094 (7)	0.456 (17)
H113b	0.498886	0.693813	0.357604	0.113*	0.456 (17)
C114b	0.5589 (17)	0.752 (2)	0.5057 (8)	0.092 (7)	0.456 (17)
H114b	0.479659	0.682122	0.521112	0.111*	0.456 (17)
C115b	0.6630 (16)	0.841 (2)	0.5816 (9)	0.043 (4)	0.456 (17)
C116b	0.779 (2)	0.9444 (17)	0.5532 (10)	0.064 (4)	0.456 (17)
H116b	0.851599	1.011918	0.601356	0.076*	0.456 (17)
C117b	0.7812 (19)	0.9422 (19)	0.4510 (10)	0.063 (5)	0.456 (17)
H117b	0.865749	1.000082	0.432854	0.076*	0.456 (17)
C118b	0.653 (3)	0.832 (3)	0.6879 (11)	0.054 (6)	0.456 (17)
H118b	0.561079	0.786706	0.702699	0.065*	0.456 (17)
C19	0.7642 (5)	0.8832 (5)	0.7661 (3)	0.0506 (10)	
H19a	0.856178	0.892861	0.749447	0.061*	0.544 (17)
H19Ab	0.857626	0.926208	0.752932	0.061*	0.456 (17)
C20	0.7444 (4)	0.8739 (5)	0.8704 (3)	0.0468 (9)	
C21	0.6174 (5)	0.8778 (5)	0.9068 (3)	0.0517 (10)	
H21	0.539662	0.883691	0.863557	0.062*	
C22	0.6070 (5)	0.8729 (5)	1.0051 (3)	0.0512 (10)	
H22	0.520791	0.875931	1.026875	0.061*	
C23	0.8363 (4)	0.8605 (4)	1.0386 (3)	0.0462 (9)	
H23	0.912659	0.855557	1.083746	0.055*	
C24	0.8546 (5)	0.8638 (5)	0.9401 (3)	0.0486 (9)	
H24	0.941229	0.859288	0.919813	0.058*	
C25	0.532 (4)	0.489 (3)	0.613 (3)	0.115 (10)	0.205 (7)
H25	0.469078	0.488621	0.659763	0.138*	0.205 (7)
O5	0.653 (4)	0.486 (4)	0.638 (3)	0.158 (12)	0.205 (7)
N4	0.488 (4)	0.494 (4)	0.517 (3)	0.120 (9)	0.205 (7)
C26	0.339 (4)	0.500 (5)	0.496 (4)	0.124 (11)	0.205 (7)
H26A	0.285901	0.468594	0.548200	0.186*	0.205 (7)
H26B	0.290252	0.438990	0.432179	0.186*	0.205 (7)
H26C	0.343390	0.597964	0.492258	0.186*	0.205 (7)
C27	0.571 (6)	0.498 (6)	0.434 (4)	0.147 (15)	0.205 (7)
H27A	0.519568	0.419088	0.380124	0.221*	0.205 (7)
H27B	0.664506	0.490555	0.457324	0.221*	0.205 (7)
H27C	0.584640	0.587607	0.410528	0.221*	0.205 (7)

Atomic displacement parameters (Å²)

	U^{11}	U^{22}	U^{33}	U^{12}	U^{13}	U^{23}
Ni1	0.0410 (4)	0.0368 (4)	0.0366 (4)	0.0120 (3)	0.0031 (2)	0.0118 (2)
S1	0.0459 (6)	0.0397 (5)	0.0669 (7)	0.0161 (4)	0.0007 (4)	0.0156 (4)
O1	0.0501 (16)	0.0438 (15)	0.0586 (17)	0.0175 (12)	0.0002 (13)	0.0154 (12)
O2	0.0541 (19)	0.0419 (17)	0.122 (3)	0.0139 (15)	0.0082 (19)	0.0239 (18)
O3	0.0405 (15)	0.0428 (14)	0.0574 (16)	0.0143 (12)	0.0012 (12)	0.0118 (12)
O4	0.0429 (14)	0.0370 (13)	0.0607 (17)	0.0163 (11)	0.0027 (12)	0.0152 (12)
N1	0.0434 (17)	0.0473 (18)	0.0438 (17)	0.0093 (14)	0.0025 (14)	0.0148 (14)
N3	0.0473 (18)	0.0440 (17)	0.0391 (16)	0.0176 (14)	0.0055 (13)	0.0139 (13)

C1	0.053 (2)	0.041 (2)	0.053 (2)	0.0175 (18)	0.0045 (18)	0.0138 (17)
C2	0.051 (2)	0.041 (2)	0.066 (3)	0.0169 (18)	0.0047 (19)	0.0168 (18)
C3	0.049 (3)	0.043 (2)	0.129 (5)	0.011 (2)	-0.005 (3)	0.027 (3)
C4	0.052 (3)	0.044 (2)	0.127 (5)	0.019 (2)	-0.005 (3)	0.024 (3)
C5	0.049 (2)	0.036 (2)	0.072 (3)	0.0162 (17)	0.004 (2)	0.0154 (18)
C6	0.045 (2)	0.0387 (19)	0.047 (2)	0.0141 (16)	0.0049 (16)	0.0112 (16)
C7	0.048 (2)	0.060 (3)	0.049 (2)	0.015 (2)	0.0038 (18)	0.0068 (19)
C8	0.048 (2)	0.077 (3)	0.070 (3)	0.021 (2)	0.004 (2)	0.018 (3)
C9	0.055 (3)	0.059 (3)	0.055 (3)	0.006 (2)	-0.007 (2)	0.008 (2)
C10	0.062 (3)	0.057 (3)	0.089 (4)	0.012 (2)	-0.010 (3)	-0.001 (3)
C11	0.049 (2)	0.045 (2)	0.076 (3)	0.0095 (19)	-0.006 (2)	0.002 (2)
C12	0.055 (3)	0.066 (3)	0.075 (3)	0.014 (2)	-0.003 (2)	0.004 (2)
N2a	0.038 (9)	0.088 (12)	0.020 (6)	0.021 (7)	0.006 (5)	0.004 (6)
C13a	0.059 (6)	0.134 (13)	0.042 (5)	0.047 (7)	0.005 (4)	0.022 (6)
C14a	0.051 (5)	0.158 (15)	0.042 (5)	0.047 (7)	0.013 (4)	0.023 (6)
C15a	0.055 (7)	0.056 (11)	0.038 (5)	0.017 (6)	0.002 (4)	0.007 (5)
C16a	0.044 (5)	0.072 (8)	0.039 (5)	0.024 (5)	0.005 (3)	0.016 (5)
C17a	0.044 (5)	0.075 (9)	0.044 (5)	0.022 (5)	0.008 (4)	0.019 (5)
C18a	0.048 (7)	0.062 (12)	0.047 (6)	0.022 (7)	0.011 (4)	0.010 (5)
N12b	0.060 (15)	0.046 (10)	0.068 (14)	0.009 (8)	0.001 (10)	0.028 (8)
C113b	0.082 (9)	0.111 (14)	0.041 (6)	-0.032 (9)	-0.007 (6)	0.016 (7)
C114b	0.082 (9)	0.108 (14)	0.047 (6)	-0.027 (9)	-0.006 (6)	0.027 (7)
C115b	0.048 (7)	0.050 (11)	0.030 (6)	0.012 (5)	0.006 (4)	0.011 (5)
C116b	0.071 (10)	0.063 (9)	0.044 (6)	0.008 (7)	-0.002 (6)	0.009 (6)
C117b	0.058 (8)	0.075 (11)	0.046 (7)	0.001 (7)	0.011 (6)	0.021 (7)
C118b	0.062 (8)	0.064 (15)	0.031 (6)	0.007 (9)	0.009 (5)	0.017 (6)
C19	0.052 (2)	0.064 (3)	0.038 (2)	0.020 (2)	0.0086 (17)	0.0131 (18)
C20	0.048 (2)	0.052 (2)	0.040 (2)	0.0163 (18)	0.0068 (16)	0.0120 (17)
C21	0.049 (2)	0.070 (3)	0.042 (2)	0.025 (2)	0.0068 (17)	0.0194 (19)
C22	0.049 (2)	0.069 (3)	0.045 (2)	0.027 (2)	0.0090 (17)	0.0205 (19)
C23	0.044 (2)	0.051 (2)	0.043 (2)	0.0150 (17)	0.0024 (16)	0.0128 (17)
C24	0.047 (2)	0.058 (2)	0.042 (2)	0.0177 (19)	0.0074 (17)	0.0123 (18)
C25	0.121 (12)	0.103 (14)	0.120 (12)	0.033 (9)	0.022 (8)	0.019 (9)
O5	0.135 (14)	0.16 (2)	0.167 (19)	0.046 (14)	0.010 (12)	0.026 (15)
N4	0.125 (12)	0.109 (13)	0.118 (11)	0.028 (9)	0.024 (7)	0.013 (9)
C26	0.134 (14)	0.103 (19)	0.124 (19)	0.027 (15)	0.008 (12)	0.020 (16)
C27	0.16 (2)	0.14 (2)	0.139 (18)	0.033 (16)	0.046 (16)	0.030 (16)

Geometric parameters (Å, °)

Ni1—O1	2.017 (3)	C14a—H14a	0.9300
Ni1—O3 ⁱ	2.156 (3)	C14a—C15a	1.364 (13)
Ni1—O4 ⁱ	2.144 (3)	C15a—C16a	1.396 (14)
Ni1—N1	2.094 (3)	C15a—C18a	1.467 (11)
Ni1—N3 ⁱⁱ	2.112 (3)	C16a—H16a	0.9300
Ni1—C6 ⁱ	2.472 (4)	C16a—C17a	1.383 (11)
Ni1—N2	2.109 (9)	C17a—H17a	0.9300
Ni1—N12b	2.079 (15)	C18a—H18a	0.9300

S1—C2	1.721 (4)	C18a—C19	1.31 (2)
S1—C5	1.714 (4)	N12b—C113b	1.371 (14)
O1—C1	1.264 (5)	N12b—C117b	1.300 (14)
O2—C1	1.236 (5)	C113b—H113b	0.9300
O3—Ni1 ⁱⁱⁱ	2.156 (3)	C113b—C114b	1.363 (12)
O3—C6	1.266 (5)	C114b—H114b	0.9300
O4—Ni1 ⁱⁱⁱ	2.144 (3)	C114b—C115b	1.359 (14)
O4—C6	1.268 (5)	C115b—C116b	1.401 (14)
N1—C7	1.325 (6)	C115b—C118b	1.470 (11)
N1—C11	1.347 (6)	C116b—H116b	0.9300
N3—Ni1 ^{iv}	2.112 (3)	C116b—C117b	1.387 (13)
N3—C22	1.341 (5)	C117b—H117b	0.9300
N3—C23	1.347 (5)	C118b—H118b	0.9300
C1—C2	1.488 (5)	C118b—C19	1.35 (2)
C2—C3	1.349 (6)	C19—H19a	0.9300
C3—H3	0.9300	C19—H19Ab	0.9300
C3—C4	1.414 (6)	C19—C20	1.461 (5)
C4—H4	0.9300	C20—C21	1.393 (6)
C4—C5	1.347 (6)	C20—C24	1.391 (6)
C5—C6	1.476 (5)	C21—H21	0.9300
C6—Ni1 ⁱⁱⁱ	2.472 (4)	C21—C22	1.355 (6)
C7—H7	0.9300	C22—H22	0.9300
C7—C8	1.381 (6)	C23—H23	0.9300
C8—H8	0.9300	C23—C24	1.370 (5)
C8—C9	1.393 (7)	C24—H24	0.9300
C9—C10	1.363 (7)	C25—H25	0.9300
C9—C12	1.486 (6)	C25—O5	1.213 (19)
C10—H10	0.9300	C25—N4	1.34 (2)
C10—C11	1.366 (7)	N4—C26	1.47 (2)
C11—H11	0.9300	N4—C27	1.46 (2)
C12—C12 ^v	1.290 (10)	C26—H26A	0.9600
C12—H12	0.9300	C26—H26B	0.9600
N2a—C13a	1.352 (8)	C26—H26C	0.9600
N2a—C17a	1.323 (8)	C27—H27A	0.9600
C13a—H13a	0.9300	C27—H27B	0.9600
C13a—C14a	1.355 (11)	C27—H27C	0.9600
O1—Ni1—O3 ⁱ	172.16 (11)	N2a—C13a—H13a	118.3
O1—Ni1—O4 ⁱ	110.62 (11)	N2a—C13a—C14a	123.4 (8)
O1—Ni1—N1	90.21 (13)	C14a—C13a—H13a	118.3
O1—Ni1—N3 ⁱⁱ	91.18 (12)	C13a—C14a—H14a	119.6
O1—Ni1—C6 ⁱ	141.40 (13)	C13a—C14a—C15a	120.8 (9)
O1—Ni1—N2a	90.2 (5)	C15a—C14a—H14a	119.6
O1—Ni1—N12b	90.1 (5)	C14a—C15a—C16a	116.4 (10)
O3 ⁱ —Ni1—C6 ⁱ	30.80 (12)	C14a—C15a—C18a	120.5 (13)
O4 ⁱ —Ni1—O3 ⁱ	61.62 (10)	C16a—C15a—C18a	122.4 (13)
O4 ⁱ —Ni1—C6 ⁱ	30.85 (11)	C15a—C16a—H16a	120.4
N1—Ni1—O3 ⁱ	97.44 (12)	C17a—C16a—C15a	119.1 (9)

N1—Ni1—O4 ⁱ	158.61 (12)	C17a—C16a—H16a	120.4
N1—Ni1—N3 ⁱⁱ	87.44 (13)	N2a—C17a—C16a	123.9 (10)
N1—Ni1—C6 ⁱ	127.99 (13)	N2a—C17a—H17a	118.1
N1—Ni1—N2a	95.7 (3)	C16a—C17a—H17a	118.1
N3 ⁱⁱ —Ni1—O3 ⁱ	87.47 (12)	C15a—C18a—H18a	116.6
N3 ⁱⁱ —Ni1—O4 ⁱ	87.32 (12)	C19—C18a—C15a	126.8 (16)
N3 ⁱⁱ —Ni1—C6 ⁱ	85.91 (13)	C19—C18a—H18a	116.6
N2a—Ni1—O3 ⁱ	90.7 (5)	C113b—N12b—Ni1	120.4 (11)
N2a—Ni1—O4 ⁱ	89.2 (4)	C117b—N12b—Ni1	123.5 (10)
N2a—Ni1—N3 ⁱⁱ	176.6 (4)	C117b—N12b—C113b	113.9 (12)
N2a—Ni1—C6 ⁱ	91.0 (5)	N12b—C113b—H113b	118.3
N12b—Ni1—O3 ⁱ	91.1 (5)	C114b—C113b—N12b	123.4 (11)
N12b—Ni1—O4 ⁱ	91.1 (4)	C114b—C113b—H113b	118.3
N12b—Ni1—N1	93.8 (4)	C113b—C114b—H114b	119.5
N12b—Ni1—N3 ⁱⁱ	178.3 (5)	C115b—C114b—C113b	121.0 (11)
N12b—Ni1—C6 ⁱ	92.4 (5)	C115b—C114b—H114b	119.5
C5—S1—C2	91.8 (2)	C114b—C115b—C116b	116.6 (11)
C1—O1—Ni1	125.3 (3)	C114b—C115b—C118b	121.4 (14)
C6—O3—Ni1 ⁱⁱⁱ	88.5 (2)	C116b—C115b—C118b	122.0 (13)
C6—O4—Ni1 ⁱⁱⁱ	89.0 (2)	C115b—C116b—H116b	121.1
C7—N1—Ni1	122.3 (3)	C117b—C116b—C115b	117.9 (12)
C7—N1—C11	116.5 (4)	C117b—C116b—H116b	121.1
C11—N1—Ni1	119.3 (3)	N12b—C117b—C116b	126.0 (13)
C22—N3—Ni1 ^{iv}	122.7 (3)	N12b—C117b—H117b	117.0
C22—N3—C23	116.0 (3)	C116b—C117b—H117b	117.0
C23—N3—Ni1 ^{iv}	121.2 (3)	C115b—C118b—H118b	116.9
O1—C1—C2	115.4 (4)	C19—C118b—C115b	126.3 (19)
O2—C1—O1	126.2 (4)	C19—C118b—H118b	116.9
O2—C1—C2	118.3 (4)	C18a—C19—H19a	117.9
C1—C2—S1	121.0 (3)	C18a—C19—C20	124.2 (8)
C3—C2—S1	111.0 (3)	C118b—C19—H19Ab	118.5
C3—C2—C1	127.9 (4)	C118b—C19—C20	123.0 (9)
C2—C3—H3	123.6	C20—C19—H19a	117.9
C2—C3—C4	112.9 (4)	C20—C19—H19Ab	118.5
C4—C3—H3	123.6	C21—C20—C19	122.8 (4)
C3—C4—H4	123.4	C24—C20—C19	121.2 (4)
C5—C4—C3	113.1 (4)	C24—C20—C21	116.0 (4)
C5—C4—H4	123.4	C20—C21—H21	119.9
C4—C5—S1	111.2 (3)	C22—C21—C20	120.1 (4)
C4—C5—C6	127.3 (4)	C22—C21—H21	119.9
C6—C5—S1	121.4 (3)	N3—C22—C21	124.3 (4)
O3—C6—Ni1 ⁱⁱⁱ	60.67 (19)	N3—C22—H22	117.8
O3—C6—O4	120.7 (3)	C21—C22—H22	117.8
O3—C6—C5	120.6 (3)	N3—C23—H23	118.5
O4—C6—Ni1 ⁱⁱⁱ	60.12 (19)	N3—C23—C24	123.1 (4)
O4—C6—C5	118.7 (4)	C24—C23—H23	118.5
C5—C6—Ni1 ⁱⁱⁱ	176.5 (3)	C20—C24—H24	119.8
N1—C7—H7	118.2	C23—C24—C20	120.5 (4)

N1—C7—C8	123.5 (4)	C23—C24—H24	119.8
C8—C7—H7	118.2	O5—C25—H25	120.0
C7—C8—H8	120.3	O5—C25—N4	120 (4)
C7—C8—C9	119.4 (5)	N4—C25—H25	120.0
C9—C8—H8	120.3	C25—N4—C26	115 (3)
C8—C9—C12	124.6 (5)	C25—N4—C27	127 (4)
C10—C9—C8	116.7 (4)	C27—N4—C26	118 (4)
C10—C9—C12	118.7 (5)	N4—C26—H26A	109.5
C9—C10—H10	119.6	N4—C26—H26B	109.5
C9—C10—C11	120.8 (5)	N4—C26—H26C	109.5
C11—C10—H10	119.6	H26A—C26—H26B	109.5
N1—C11—C10	123.1 (5)	H26A—C26—H26C	109.5
N1—C11—H11	118.4	H26B—C26—H26C	109.5
C10—C11—H11	118.4	N4—C27—H27A	109.5
C9—C12—H12	117.2	N4—C27—H27B	109.5
C12 ^v —C12—C9	125.6 (7)	N4—C27—H27C	109.5
C12 ^v —C12—H12	117.2	H27A—C27—H27B	109.5
C13a—N2a—Ni1	123.1 (8)	H27A—C27—H27C	109.5
C17a—N2a—Ni1	121.1 (7)	H27B—C27—H27C	109.5
C17a—N2a—C13a	115.5 (9)		
Ni1—O1—C1—O2	-14.6 (7)	C10—C9—C12—C12 ^v	175.1 (8)
Ni1—O1—C1—C2	167.8 (3)	C11—N1—C7—C8	-0.5 (7)
Ni1 ⁱⁱⁱ —O3—C6—O4	-3.5 (4)	C12—C9—C10—C11	179.0 (5)
Ni1 ⁱⁱⁱ —O3—C6—C5	176.2 (4)	N2a—C13a—C14a—C15a	9 (3)
Ni1 ⁱⁱⁱ —O4—C6—O3	3.6 (4)	C13a—N2a—C17a—C16a	9 (2)
Ni1 ⁱⁱⁱ —O4—C6—C5	-176.2 (4)	C13a—C14a—C15a—C16a	-5 (3)
Ni1—N1—C7—C8	163.5 (4)	C13a—C14a—C15a—C18a	-176.3 (15)
Ni1—N1—C11—C10	-163.1 (4)	C14a—C15a—C16a—C17a	4 (2)
Ni1 ^{iv} —N3—C22—C21	178.4 (4)	C14a—C15a—C18a—C19	176.7 (16)
Ni1 ^{iv} —N3—C23—C24	-179.0 (3)	C15a—C16a—C17a—N2a	-6 (2)
Ni1—N2a—C13a—C14a	176.4 (12)	C15a—C18a—C19—C20	179.3 (13)
Ni1—N2a—C17a—C16a	-177.7 (11)	C16a—C15a—C18a—C19	6 (3)
Ni1—N12b—C113b—C114b	174.4 (16)	C17a—N2a—C13a—C14a	-10 (2)
Ni1—N12b—C117b—C116b	-176.8 (14)	C18a—C15a—C16a—C17a	174.6 (14)
S1—C2—C3—C4	-0.7 (7)	C18a—C19—C20—C21	-8.4 (13)
S1—C5—C6—O3	-7.8 (6)	C18a—C19—C20—C24	173.0 (11)
S1—C5—C6—O4	172.0 (3)	N12b—C113b—C114b—C115b	-5 (3)
O1—C1—C2—S1	4.6 (6)	C113b—N12b—C117b—C116b	-13 (3)
O1—C1—C2—C3	-178.1 (5)	C113b—C114b—C115b—C116b	1 (3)
O2—C1—C2—S1	-173.2 (4)	C113b—C114b—C115b—C118b	180 (2)
O2—C1—C2—C3	4.1 (8)	C114b—C115b—C116b—C117b	-3 (3)
N1—C7—C8—C9	-0.6 (8)	C114b—C115b—C118b—C19	160 (2)
N3—C23—C24—C20	1.2 (7)	C115b—C116b—C117b—N12b	10 (3)
C1—C2—C3—C4	-178.2 (5)	C115b—C118b—C19—C20	177.9 (16)
C2—S1—C5—C4	-1.1 (5)	C116b—C115b—C118b—C19	-21 (3)
C2—S1—C5—C6	179.7 (4)	C117b—N12b—C113b—C114b	10 (3)
C2—C3—C4—C5	-0.1 (8)	C118b—C115b—C116b—C117b	178.2 (19)

C3—C4—C5—S1	0.9 (7)	C118b—C19—C20—C21	-31.1 (15)
C3—C4—C5—C6	180.0 (5)	C118b—C19—C20—C24	150.4 (14)
C4—C5—C6—O3	173.2 (5)	C19—C20—C21—C22	-178.1 (4)
C4—C5—C6—O4	-7.1 (8)	C19—C20—C24—C23	177.6 (4)
C5—S1—C2—C1	178.7 (4)	C20—C21—C22—N3	-0.2 (7)
C5—S1—C2—C3	1.0 (5)	C21—C20—C24—C23	-1.0 (6)
C7—N1—C11—C10	1.3 (7)	C22—N3—C23—C24	-0.8 (6)
C7—C8—C9—C10	0.9 (8)	C23—N3—C22—C21	0.3 (7)
C7—C8—C9—C12	-178.2 (5)	C24—C20—C21—C22	0.5 (7)
C8—C9—C10—C11	-0.1 (8)	O5—C25—N4—C26	-179 (3)
C8—C9—C12—C12 ^v	-5.8 (11)	O5—C25—N4—C27	-1 (3)
C9—C10—C11—N1	-1.1 (9)		

Symmetry codes: (i) $x, y+1, z$; (ii) $x, y, z-1$; (iii) $x, y-1, z$; (iv) $x, y, z+1$; (v) $-x, -y+1, -z$.

Hydrogen-bond geometry (\AA , $^\circ$)

$Cg1$, $Cg2$ and $Cg3$ are the centroids of rings (N2A,C13A–C17A), (N3,C20–C24) and (N1,C7–C11), respectively.

$D-H\cdots A$	$D-H$	$H\cdots A$	$D\cdots A$	$D-H\cdots A$
C8—H8 \cdots O2 ^{vi}	0.93	2.59	3.314 (7)	135
C19—H19A \cdots O4 ^{vii}	0.93	2.51	3.430 (6)	169
C21—H21 \cdots O3 ^{viii}	0.93	2.41	3.331 (6)	171
C27—H27C \cdots Cg1	0.96	2.78	3.57 (6)	140
C10—H10 \cdots Cg2 ^{viii}	0.93	2.88	3.696 (6)	147
C22—H22 \cdots Cg3 ^{iv}	0.93	2.93	3.534 (5)	124

Symmetry codes: (iv) $x, y, z+1$; (vi) $x-1, y, z$; (vii) $-x+2, -y+1, -z+1$; (viii) $-x+1, -y+1, -z+1$.